Therefore in the spectral analyses of the $Rh_x(O_2)_y$ complexes these "impurity lines" were not considered.

Registry No. $Rh(^{16}O_2)_2$, 63904-17-6; $Rh(^{16}O_2)(^{16}O^{18}O)$, 63884-20-8; $Rh(^{16}O^{18}O)_2$, 63884-19-5; $Rh(^{18}O_2)(^{16}O_2)$, 63866-48-8; $Rh(^{18}O_2)(^{16}O^{18}O)$, 63884-18-4; $Rh(^{18}O_2)_2$, 63866-47-7; $Rh(^{16}O_2)$, 63884-17-3; $Rh(^{16}O^{18}O)$, 63884-16-2; $Rh(^{18}O_2)$, 63848-54-4; Rh, 7440-16-6; Rh_2, 12596-98-4; $Pd(O_2)_2$, 63848-53-3.

References and Notes

(1) (a) G. A. Ozin, *Acc. Chem. Res.*, **10**, 21 (1977); *Catal. Rev.*, in press; (b) H. Huber, G. A. Ozin, and W. J. Power, *J. Am. Chem. Soc.*, **98**, 6508 (1976); W. J. Power and G. A. Ozin, *Inorg. Chem.*, **16**, 212 (1977); (c) D. McIntosh and G. A. Ozin, *Inorg. Chem.*, 16, 59 (1977); H. Huber and G. A. Ozin, *ibid.*, **16**, 64 (1977); (d) R. Ugo, *Catal. Rev.*, **11**, 225 (1975); E. L. Muetterties, *Bull. Soc. Chim. Belg.*, **84**, 959 (1975); K. H. Johnson and R. P. Messmer, *J. Vac. Sci. Technol.*, **11**, 236 (1975), and references therein.

(2) A. J. L. Hanlan and G. A. Ozin, *Inorg. Chem.*, following paper in this issue.

(3) See for example N. W. Cant and W. K. Hall, *J. Catal.*, **16**, 220 (1970); **27**, 70 (1972), and references therein.

(4) N. W. Cant and W. K. Hall, *J. Catal.*, **23**, 287, (1971); *J. Phys. Chem.*, **75**, 2914 (1971), and references therein.

(5) E. P. Kündig, M. Moskovits, and G. A. Ozin, *J. Mol. Struct.*, **14**, 137 (1972).

(6) M. Moskovits and G. A. Ozin, *J. Appl. Spectrosc.*, **26**, 487 (1972).

(7) G. A. Ozin and A. Vander Voet, *Can. J. Chem.*, **51**, 3332 (1973).

(8) L. A. Hanlan and G. A. Ozin, *J. Am. Chem. Soc.*, **96**, 6324 (1974).

(9) E. P. Kündig, M. Moskovits, and G. A. Ozin, *Nature (London)*, **254**, 503 (1975).

(10) H. Huber, E. P. Kündig, G. A. Ozin, and A. J. Poe, *J. Am. Chem. Soc.*, **97**, 308 (1975); H. Huber, E. P. Kündig, M. Moskovits, and G. A. Ozin, *ibid.*, **97**, 2097 (1975); E. P. Kündig, M. Moskovits, and G. A. Ozin, *Angew. Chem., Int. Ed. Engl.*, **14**, 292 (1975), and references therein.

(11) R. Busby, W. Klotzbücher, and G. A. Ozin, *J. Am. Chem. Soc.*, **98**, 4013 (1976).

(12) T. A. Ford, E. P. Kündig, W. Klotzbücher, M. Moskovits, and G. A. Ozin, *J. Chem. Phys.*, **66**, 524 (1977).

(13) (a) T. C. DeVore, A. Ewing, H. F. Franzen, and V. Calder, *Chem. Phys. Lett.*, **35**, 78 (1975); (b) H. Huber, G. A. Ozin, and W. J. Power, *J. Am. Chem. Soc.*, **98**, 6508 (1976); (c) J. Hulse and M. Moskovits, *J. Chem. Phys.*, **66**, 3988 (1977).

(14) E. P. Kündig, M. Moskovits, and G. A. Ozin, *J. Am. Chem. Soc.*, **97**, 2097 (1975); G. A. Ozin, *Appl. Spectrosc.*, **30**, 573 (1976).

(15) W. Klotzbücher and G. A. Ozin, *Inorg. Chem.*, **16**, 984 (1977).

(16) C. Moore, *Natl. Bur. Stand. (U.S.), Monogr.*, **No. 53** (1962).

(17) J. M. Brom, Jr., W. R. M. Graham, and W. Weltner, Jr., *J. Chem. Phys.*, **57**, 4116 (1972).

(18) D. M. Mann and H. P. Broida, *J. Chem. Phys.*, **55**, 84 (1971); L. Brewer and C. Chang, *ibid.*, **56** (1972); D. M. Green and D. H. W. Carstens, *ibid.*, **54**, 5206 (1971); W. Klotzbücher and G. A. Ozin, *Inorg. Chem.*, **15**, 292 (1976); D. H. W. Carstens, W. Brashear, D. R. Eslinger, and D. M. Gruen, *Appl. Spectrosc.*, **26**, 184 (1972). See D. M. Gruen in "Cryochemistry", M. Moskovits and G. A. Ozin, Ed., Wiley, New York, N.Y., 1976, for detailed discussions of "matrix-induced frequency shifts".

(19) W. F. Cooper, G. A. Clarke, and C. R. Hare, *J. Phys. Chem.*, **76**, 2268 (1972); P. Joyes and M. Leleyter, *J. Phys. B*, **6**, 150 (1973); R. P. Messmer, S. K. Knudson, K. H. Johnson, J. B. Diamond, and C. Y. Yang, *Phys. Rev. B*, **13**, 1396 (1976); C. F. Melius, J. W. Moskowitz, A. P. Mortola, M. B. Baillie, and M. A. Ratner, *Surf. Sci.*, **54**, 279 (1976); W. A. Goddard III and T. Upton, *J. Am. Chem. Soc.*, in press (and private communication), and references therein.

(20) H. Huber, W. Klotzbücher, G. A. Ozin, and A. Vander Voet, *Can. J. Chem.*, **51**, 2722 (1973).

(21) (a) J. S. Darling, M. B. Garton-Sprenger, and J. S. Ogden, *Faraday Soc. Symp.*, **8**, 75 (1973). (b) Note that a detailed electronic spectral examination of binary $M(O_2)_2$ complexes (M = Ti, V, Cr, Mn, Fe, Co, Ni, Cu) indicate that an end-on superoxide formulation might be more appropriate: H. B. Gray, A. B. P. Lever, and G. A. Ozin, in preparation.

(22) L. Vaska, *Acc. Chem. Res.*, **9**, 175 (1976).

(23) L. Andrews, *J. Mol. Spectrosc.*, **61**, 337 (1976), and references therein.

(24) M. A. Bennett and P. A. Longstaff, *J. Am. Chem. Soc.*, **91**, 6266 (1969), and C. Masters and B. L. Shaw, *J. Chem. Soc. A*, 3678 (1971).

(25) See for example W. Klotzbücher and G. A. Ozin, *Inorg. Chem.*, **15**, 292 (1976).

(26) G. A. Ozin and A. Vander Voet, *Can. J. Chem.*, **51**, 3332 (1973).

(27) W. Klotzbücher and G. A. Ozin, *J. Am. Chem. Soc.*, **97**, 3765 (1975).

(28) Trace impurities can originate from (i) the walls of the vacuum system, (ii) the matrix gases themselves, (iii) small air leaks in the vacuum system, and (iv) the trace carbon content of the metal vapor source reacting with trace amounts of dioxygen to yield CO and/or CO_2.

(29) W. Klotzbücher, G. A. Ozin, J. G. Norman, Jr., and H. Kolari, *Inorg. Chem.*, **16**, 2871 (1977).

(30) W. Klotzbücher and G. A. Ozin, *J. Mol. Catal.*, in press, and paper presented at the meeting "Relationships between Homogeneous and Heterogeneous Catalysis", Lyon, Nov 1977.

(31) H. Huber and G. A. Ozin, *Inorg. Chem.*, in press, and paper presented at the meeting "Matrix Isolation Spectroscopy", West Berlin, June 1977; W. Schulze, H. U. Becker, and H. Abe, paper presented at the same conference.

Contribution from the Lash Miller Chemistry Laboratory and Erindale College,
University of Toronto, Toronto, Ontario, Canada

Rhodium Atom Chemistry. 2. Interaction of Small, Well-Defined Rhodium Clusters with Dioxygen. $Rh_2(O_2)_n$ and $Rh_3(O_2)_m$, Localized Bonding Models for Dioxygen Chemisorption on Rhodium Metal

A. J. LEE HANLAN and GEOFFREY A. OZIN*

Received January 11, 1977 AIC70012I

The interaction of small, well-defined rhodium clusters, Rh_n (where $n = 2$ or 3), with molecular dioxygen has been investigated for the first time by matrix infrared and UV–visible spectroscopy coupled with metal/dioxygen concentration experiments, warmup studies, and dioxygen isotopic substitution techniques. A number of binuclear dioxygen complexes of the type $Rh_2(O_2)_n$ (where $n = 1, 2, 3,$ or 4) together with a trinuclear $Rh_3(O_2)_m$ (where m is probably 2 or 6) have been identified and characterized spectroscopically. The properties of these complexes are most intriguing. $Rh_2(O_2)_4$, for example, can be considered to be the metal–metal bonded dimer of the parent monomer $Rh(O_2)_2$, the latter having been defined in part 1 of this study. Moreover, the $Rh_2(O_2)_{1-3}$ reactive intermediates can be visualized as being derived from $Rh_2(O_2)_4$ by successive dioxygen stripping. It would also appear that the highest stoichiometry trimer complex $Rh_3(O_2)_n$ is also derived from $Rh(O_2)_2$ and is probably best described as a triangular metal cluster of three "$Rh(O_2)_2$" units. In addition to these binuclear and trinuclear cluster compounds containing dioxygen ligands with oxygen–oxygen stretching frequencies in the range normally expected for coordinated $O_2^{\delta-}$ (ν(OO) 1150–850 cm^{-1} for $1 \leq \delta \leq 2$), there also exists a fascinating binuclear $Rh_2(O_2)$ complex which exhibits an unprecedentedly high oxygen–oxygen stretching mode at 1275–1265 cm^{-1}. All of the cluster complexes described, together with their mononuclear counterpart complexes $Rh(O_2)_{1,2}$, are considered in this paper to be useful localized bonding models for probing the chemisorbed state of dioxygen on rhodium metal surfaces and are discussed in terms of their possible relevance to some heterogeneous oxidation catalysis involving olefins.

Introduction

The past decade has witnessed a renaissance in surface crystallography and surface spectroscopy to the point that reliable microscopic information is almost becoming routinely available on the interaction between transition metal surfaces and a variety of atoms and molecules.[1a] In both theoretical[1b] and experimental[1c] studies of chemisorption and catalysis, a great deal of discussion has focused on the validity of employing localized models for elucidating the surface bonding between adsorbate and adsorbent.[1b-d] For this model the chemisorption bond is described in terms of a surface atom or molecule, by coupling the adsorbent wave functions to only a limited number of neighboring surface atoms.[1b-d] In an attempt to ascertain which classes of compound can provide realistic models of metal surfaces for chemisorption and heterogeneous catalysis studies, both mononuclear and discrete metal cluster compounds have been evaluated.[1] However, one of the shortcomings of comparing discrete (coordinatively saturated) complexes to surface molecules is that the former can usually only be considered as models of the surface structure of a metal where there is extensive chemisorption. Although this situation may reflect the properties of a metal surface at high surface coverage, it may not be a suitable model for submonolayer chemisorption. Analogies with model compounds are usually only justifiable if the model itself is meaningful and well defined. Up to very recently the models, whether mononuclear or cluster compounds, have usually been highly substituted by ligand atoms, ions, or molecules.[1d] It could be argued that a more valid model of the chemisorbed state is provided by a naked metal atom or naked metal cluster onto which ligands can be selectively attached in a fashion analogous to that found for the chemisorbed species on the metal surface itself. Such an idealized model would normally be inaccessible by conventional synthetic procedures because of the intrinsic activity and/or instability of these highly coordinatively unsaturated species. (We note that such lability is usually associated with reactive intermediates in a catalytic process.) However, recent developments in the cryochemical control of the reactions of metal atoms with themselves to produce small, well-defined "naked" metal clusters[2] and with other molecules to yield mononuclear and cluster reaction intermediates[3] have demonstrated the feasibility of examining these idealized, localized bonding aspects of chemisorption and catalysis. In this particular study we have investigated the interaction of small, well-defined rhodium clusters Rh_n (where $n = 2$ or 3) with molecular O_2 in an attempt to produce molecular models for evaluating the chemisorbed state of O_2 on rhodium metal surfaces and hopefully some insight into aspects of heterogeneous oxidation catalysis.

Experimental Section

See part 1 of this study.[4]

Results and Discussion

Based on the knowledge accrued from part 1[4] of this investigation concerning the facile surface diffusion and aggregation properties of Rh atoms in Ar, O_2/Ar, and O_2 matrices, it was obvious that a number of binuclear and higher cluster–dioxygen compounds were accessible for evaluation, providing their rhodium and dioxygen stoichiometries could be ascertained. In what follows a detailed account of these experiments is presented.

Dioxygen Matrices. Infrared Experiments. To establish the nature of the highest dioxygen stoichiometry rhodium cluster complexes, we studied the products of the cocondensation reaction of Rh atoms with $^{16}O_2$ at 10–12 K as a function of the Rh concentration in the range $Rh/^{16}O_2 \simeq 1/10^4$ to $1/10^2$. The results of a typical Rh concentration study are shown in Figure 1. Over the range investigated, *four* species were found to dominate the infrared spectra. These are labeled M_2 (1038 cm^{-1}), D_4 (1075 cm^{-1}), T (1130 cm^{-1}), and D_1' (1266 cm^{-1}) in Figure 1.

At low Rh concentrations the band of M_2 is favored over those of D_4, T, and D_1'. In fact T is only just observable under the low-concentration conditions. However, as the metal concentration is steadily increased, the band of M_2 displays a remarkable decrease in intensity, concomitant with increases in the relative intensities of D_4, D_1', and T (Figure 1). Recall that species M_2 has already been established in part 1 of this study to be the mononuclear bis(dioxygen)rhodium complex $Rh(O_2)_2$.[4] These results indicate that at least *three* different rhodium–dioxygen cluster complexes $Rh_x(O_2)_y$ can be easily generated in O_2 matrices in addition to the known mononuclear $Rh(O_2)_2$ (M_2).

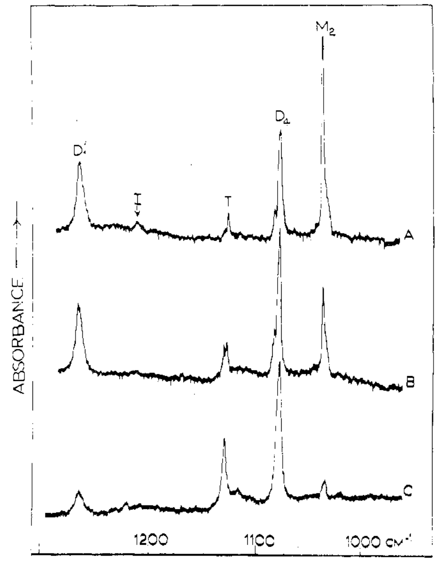

Figure 1. Infrared spectra of the products formed when Rh atoms are cocondensed with $^{16}O_2$ matrices at 10–12 K as a function of the Rh/O_2 ratio (increasing from A through C) at constant O_2 deposition rate where $M_2 = Rh(O_2)_2$, $D_4 = Rh_2(O_2)_4$, $D_1' = Rh_2(O_2)$, and $T = Rh_3(O_2)_{2\text{ or }6}$ and I shows an impurity absorption (see text for details of assignments).

The processes that are occurring in these Rh/O_2 matrix reactions can be explained in terms of either a quenched or a steady-state kinetic model of the reactions occurring within the surface regions of the matrix (the so-called reaction zone).[3,6] Binuclear and higher cluster complexes form within the reaction zone to a much greater extent than indicated by a statistical analysis based on the matrix ratio.[3,6] Our approach to establishing metal stoichiometry therefore takes advantage of the dependence of the concentration of the various species on the rate of deposition of metal. This can be calculated and compared with the observed dependence of the absorbances of bands on metal deposition rate.[3,6]

Consider a reaction network of the type

$$\begin{tikzcd}
Rh \arrow[r, "k_1"] \arrow[d, "K_1"'] & Rh(O_2) \arrow[r, "k_2"] \arrow[d, "K_1'"] & Rh(O_2)_2 \arrow[d, "K_1''"] & \\
Rh_2 \arrow[r, "k_1'"] \arrow[d, "K_2"'] & Rh_2(O_2) \arrow[r, "k_2'"] \arrow[d, "K_2'"] & Rh_2(O_2)_2 \arrow[r, "k_3'"] \arrow[d, "K_2''"] & \ldots \\
Rh_3 \arrow[r, "k_1''"] \arrow[d, "K_3"'] & Rh_3(O_2) \arrow[r, "k_2''"] \arrow[d, "K_3'"] & Rh_3(O_2)_2 \arrow[r, "k_3''"] \arrow[d, "K_3''"] & Rh_3(O\ )_3 \\
{} & {} & {} &
\end{tikzcd}$$

which is assumed to take place in the moving reaction zone during matrix deposition. One can show that, by assuming either a steady-state reaction model for the various species $Rh_x(O_2)_y$ in the moving reaction zone, or the quenched reaction model, then an expression of the type

$$[Rh_x(O_2)_y]/[Rh(O_2)_2] \propto [Rh]_0^{x-1}$$

is valid at constant metal deposition rate up to a concentration of roughly 1% total metal in the matrix. Therefore, by plotting the log of the ratio of the infrared absorbances of the suspected cluster bands D_4, D_1', and T relative to a reference mononuclear band M_2 as a function of the log of the total metal

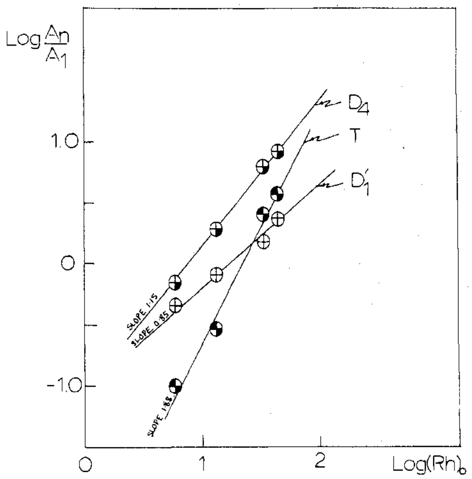

Figure 2. A log–log plot of the ratio of the absorbances of lines attributed to $Rh_x(O_2)_y$ species to that of a $Rh(O_2)_2$ reference absorption as a function of the total rhodium concentration $(Rh)_0$ at constant dioxygen deposition rate.

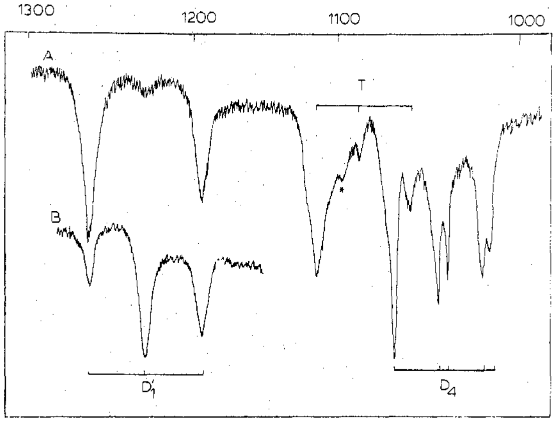

Figure 3. Matrix infrared spectrum of the products formed when Rh atoms are cocondensed with (A) $^{16}O_2/^{18}O_2 \simeq 3/2$ and (B) $^{16}O_2/^{16}O^{18}O/^{18}O_2 \simeq 1/2/1$ mixtures at 10–12 K at high $Rh/O_2 \simeq 1/(5 \times 10^2)$ ratios, showing the isotopic patterns of $D_4 = Rh_2(O_2)_4$, $D_1' = Rh_2(O_2)$ and $T = Rh_2(O_2)_{2\text{ or }6}$. Note that under these conditions $Rh(O_2)_2$ was essentially absent. (The asterisk indicates a line associated with T in $^{16}O_2$ experiments and not an $^{18}O_2$ isotope line.)

concentration $[Rh]_0$, one should obtain roughly linear plots with slopes close to "unity" for binuclears, "two" for trinuclears, and so on.[3,6]

The results of our rhodium concentration experiments in O_2 matrices are displayed in log/log form in Figure 2 from which it can be immediately deduced that species D_4 and D_1' are binuclear and T is a trinuclear species. It remains therefore to establish the dioxygen stoichiometry from oxygen isotopic labeling experiments under conditions which (i) favor maximum cluster formation, yet (ii) minimize band overlap complications. As it turns out in practice, point (ii) is difficult to achieve for species D_4 and T.

A typical infrared spectrum using $^{16}O_2/^{18}O_2 \simeq 1/2$ mixtures is displayed in Figure 3A under conditions where M_2 is essentially absent and species D_4, D_1', and T dominate. The region containing D_1' under these conditions displays an isotopic *doublet* at 1266 and 1195 cm^{-1} in place of the original single line at 1266 cm^{-1}, signifying the assignment of D_1' to a dirhodium complex containing a single dioxygen ligand, $Rh_2(O_2)$. The corresponding $^{16}O_2/^{16}O^{18}O/^{18}O_2 \simeq 1/2/1$ spectrum for D_1' (Figure 3B) shows a characteristic *triplet* isotope pattern at 1266, 1231, and 1195 cm^{-1}, the components of which have an intensity ratio of roughly 1/2/1. It would appear therefore that D_1' is best described as $Rh_2(O_2)$ containing a dioxygen moiety in which the oxygen atoms are "spectroscopically equivalent". However, as in previous studies involving $^{16}O^{18}O$ isotopic substitution,[7] one must be alert to the difficulty of resolving small splittings on the $^{16}O^{18}O$ components of coordinated dioxygen, especially for infrared absorbances with $\nu_{1/2}$ bandwidths of the order of 10 cm^{-1} as experienced with the D_1' form of $Rh_2(^{16}O^{18}O)$.

Turning our attention next to the $^{16}O_2/^{18}O_2$ isotopic structure associated with species D_4, one observes a *quintet* pattern at 1078, 1051, 1045, 1024, and 1018 cm^{-1} in place of the original line at 1078 cm^{-1} in $^{16}O_2$ matrices (Figure 3A). This type of pattern indicates that species D_4 is best formulated as a tetradioxygen complex of the form $Rh_2(O_2)_4$ and can be considered to be the dimer of the mononuclear parent species $Rh(O_2)_2$, M_2 (this point will be discussed more fully later on). Unfortunately, because of the dioxygen complexity of species D_4, it was not possible to obtain meaningful $^{16}O_2/^{16}O^{18}O/^{18}O_2$ scrambled isotopic data which might have helped establish the geometry and mode of dioxygen coordination of D_4.

The dioxygen isotopic structure associated with the trinuclear species T yields some useful information, as can be seen from the observation of at least a *triplet* pattern at 1126, 1102, and 1068 cm^{-1} in place of the original absorption at 1130 cm^{-1}. Assuming that we have not lost any isotopic information for T through band overlap with the 1078-cm^{-1} absorption of D_4 and that all of the isotopic components of T have been resolved, then one may cautiously propose a bis(dioxygen)-trirhodium formulation, $Rh_3(O_2)_2$ for species T in pure O_2 matrices.

One should note here that, if weak coupling between the dioxygen moieties prevails in the trimer, then it would be extremely difficult to distinguish $Rh_3(O_2)_2$ from, for example, $Rh_3(O_2)_6$ (see later for further discussion of this point).

We can therefore summarize our findings for Rh/O_2 cocondensations under low- and high-rhodium concentration conditions by reference to the reaction scheme shown below

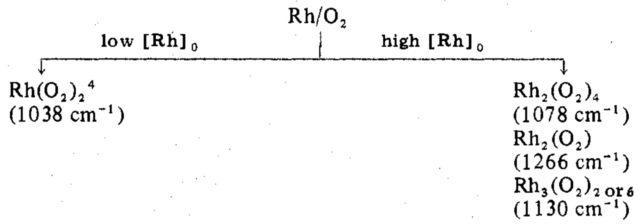

Points of interest concerning these assignments, which will be the subject of discussion at a later stage of this paper, are (i) the $\nu(OO)$ frequency ordering $Rh_3(O_2)_{2\text{ or }6} > Rh_2(O_2)_4 > Rh(O_2)_2$ and (ii) the remarkably high $\nu(OO)$ stretching frequency for the monodioxygen species $Rh_2(O_2)$, D_1'.

Dioxygen–Argon Matrix Experiments. In view of our findings in pure O_2 matrices, one might anticipate that O_2 dilution experiments in Ar would be quite complicated because of the large number of mononuclear, binuclear, trinuclear, and higher cluster complexes that are potentially accessible. Preliminary experiments in $^{16}O_2/Ar$ matrices at $Rh/Ar \simeq 1/10^3$ indicated that these fears were somewhat justified (Table I). However, the infrared spectral range over which compound formation occurred was sufficiently wide (1300–850 cm^{-1}) to make a reasonably thorough spectral and isotopic analysis worthwhile.

The regions of complexation are best divided into three ranges, 1300–1200, 1150–1000, and 950–850 cm^{-1} (Table I). Referring to the pure $^{16}O_2$ experiments described in the previous section (Table I) and the $^{16}O_2/Ar$ experiments at low Rh concentrations in part 1 of this study,[4] one can immediately identify lines which correspond reasonably closely with those ascribed to $Rh(O_2)_2$ (M_2, 1048 cm^{-1}), $Rh(O_2)$ (M_1, 908 cm^{-1}),

Table I. Observed Infrared Spectra for $Rh_x(O_2)_y$ Species Formed in O_2 and O_2/Ar Matrices

Obsd			
O_2 matrices	O_2/Ar matrices	Designation	Assignment (see text)
1266	1278 1268	D_1'	$Rh_2(O_2)$
1130	1126	T	$Rh_3(O_2)_{2\text{ or }6}$
1120 sh	1115		$Rh_3(O_2)_n$?
	1081	D_3	$Rh_2(O_2)_3$
1075	1076	D_4	$Rh_2(O_2)_4$
1038	1048	M_2	$Rh(O_2)$
	922	D_1	$Rh_2(O_2)$
	908	M_1	$Rh(O_2)$
	902	D_2	$Rh_2(O_2)_2$
	890	D_3	$Rh_2(O_2)_3$

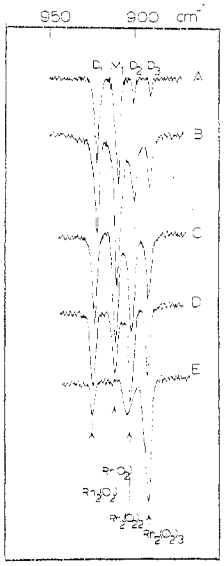

Figure 4. Infrared spectrum in the 950–850-cm^{-1} region of the products formed when Rh atoms are cocondensed with $^{16}O_2$/Ar $\simeq$ 1/50 mixtures and Rh/Ar $\simeq$ 1/10^3 (A) at 10 K, (B to E) after warmup to 20, 30, 35, and 40 K.

$Rh_2(O_2)$ (D_1', 1278 cm^{-1}), $Rh_2(O_2)_4$ (D_4, 1076 cm^{-1}), and $Rh_3(O_2)_{2\text{ or }6}$ (T, 1126 cm^{-1}). Notable, however, are *three* new absorptions in the lower ν(OO) region at 922 (D_1), 902 (D_2), and 890 (D_3) cm^{-1}. Less prominent features are observed as weak shoulders on the absorptions of D_1', T, D_4, and M_2.

Let us formalize the concentration and warmup data of a series of $^{16}O_2$/Ar experiments in the range 1/5 to 1/250. The group of new bands in the region of 900 cm^{-1} behaved in a regular and comprehensible fashion and indicated the presence of three independent species (in addition to $Rh(O_2)$, 908 cm^{-1}), D_1 (922 cm^{-1}), D_2 (902 cm^{-1}), and D_3 (890 cm^{-1}). A typical infrared spectrum on deposition and after various warmup experiments in the range 10–40 K is illustrated in Figure 4 where it can be seen that the absorption of M_1 (908 cm^{-1}) shows a slight initial increase, then steadily decays to zero at 40 K, concomitant with the growth and subsequent decay at different rates of D_1 (922 cm^{-1}) and D_2 (902 cm^{-1}). Note, however, that the absorbance of D_3 grows steadily on warming and dominates this region of the spectrum at 40 K. On the basis of the pronounced tendency of Rh_2 dimer formation in Rh/Ar $\simeq$ 1/10^3 mixtures at 10–12 K and the occurrence of the ν(OO) stretching frequencies of $D_{1,2,3}$ in the same region as that of M_1, one is tempted even at this early stage of the analysis to make an a priori assignment of $D_{1,2,3}$ to the binuclear complexes $Rh_2(O_2)_{1,2,3}$, respectively, that is, the lower stoichiometry reactive intermediates derived from "dioxygen stripping" of the parent $Rh_2(O_2)_4$, D_4 (this point will be elaborated upon later). Dioxygen concentration and warmup studies indicate that the dioxygen stoichiometry of the *three* new species absorbing in the 900-cm^{-1} region follows the order $D_3 > D_2 > D_1$.

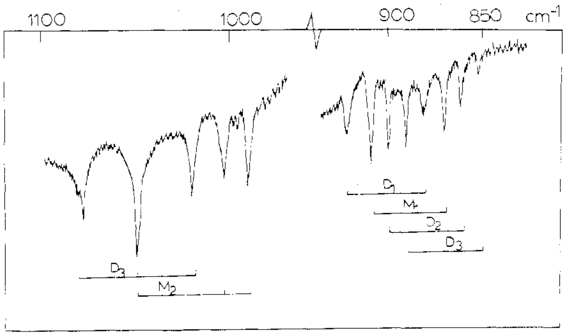

Figure 5. Infrared spectrum of the products formed when Rh atoms are cocondensed with $^{16}O_2/^{18}O_2$/Ar $\simeq$ 1/1/100 mixtures at 10–12 K with Rh/Ar $\simeq$ 1/10^3, showing the isotopic patterns associated with $D_{1,2,3}$ = $Rh_2(O_2)_{1,2,3}$ and $M_{1,2}$ = $Rh(O_2)_{1,2}$, respectively.

The corresponding experimental data in the "medium" ν(OO) frequency range is less informative and at times complicated because of small spectral splittings which appear (in most cases) to have their origin in multiple trapping site effects. One of the more striking effects observed in this region concerns the warmup behavior in the range 10–40 K. Species M_2 displays a rapid decay in absorbance, concomitant with a striking growth in the absorbances of "split" bands at 1125/1115 and 1081/1076 cm^{-1} in the regions assigned to D_4 and T. These bands grow in at different rates with respect to each other.

The growth behavior during warmup suggests that the D_3 (890 cm^{-1}) band may correspond with the 1081-cm^{-1} shoulder on the D_4 band. Any other conclusions drawn from this series of data are considered to be extremely tenuous.

The remaining feature of interest in these high-Rh concentration, O_2/Ar experiments is the remarkably high-frequency ν(OO) stretching mode at 1278 cm^{-1} which in Ar displays a weak shoulder at 1268 cm^{-1}. In this context, note that the absorption of D_1' in pure O_2 matrices occurs at 1266 cm^{-1}. On warming O_2/Ar $\simeq$ 1/5–1/50 matrices in the range 10–40 K, one observes the gradual growth of the shoulder at 1268 cm^{-1} with the simultaneous decay of the main band at 1278 cm^{-1}. This behavior may simply reflect a small matrix-induced frequency shift and splitting of D_1' in O_2/Ar or possibly the appearance of another complex related to D_1'.

Summarizing up to this point, it would appear that the following reaction scheme in O_2/Ar matrices is a reasonable description of the processes occurring at low and high Rh/Ar ratios

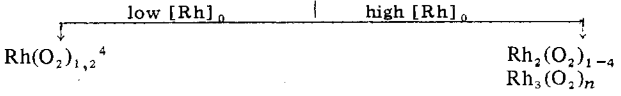

The amount of useful dioxygen isotopic substitution data that could be obtained under these dilute O_2/Ar conditions is limited by band overlap problems in most of the regions of interest. Probably our most reliable set of isotopic data concerns the dioxygen stoichiometry of species $D_{1,2,3}$ as derived from an $^{16}O_2/^{18}O_2$/Ar $\simeq$ 1/1/100 experiment (Figure 5). The 950–850-cm^{-1} region is reasonably clear-cut, showing what is probably best described as a "quartet of doublets" isotopic pattern. These *four* isotopic doublets are best ascribed to the "unique" $^{16}O_2$ and $^{18}O_2$ stretching mode of the *four* species listed in Table II, each showing an $^{16}O_2$ to $^{18}O_2$ isotopic shift of 39–40 cm^{-1}. If our association of the 1081-cm^{-1} shoulder

Table II. Observed, Low-Frequency, Infrared ν(O-O) Stretching Modes for $Rh_2(^{16}O_2)_n(^{18}O_2)_{m-n}$[a]

Molecule	$\nu(^{16}O_2)$	$\nu(^{18}O_2)$	$\Delta(\nu(^{16}O_2) - \nu(^{18}O_2))$
D_1	922	882	40
M_1	909	870	39
D_2	900	861	39
D_3	890	851	39

[a] $m = 3, n = 0\text{-}3; m = 2, n = 0\text{-}2; m = 1, n = 0\text{-}1$. Measurements in cm^{-1}.

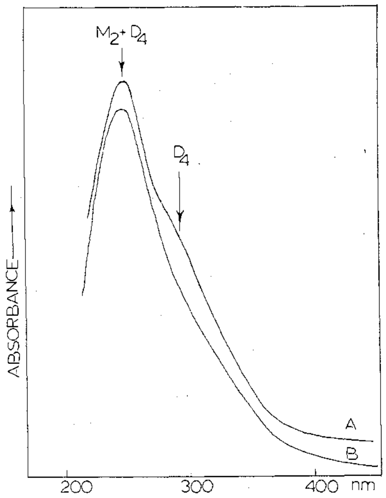

Figure 6. UV spectrum obtained on cocondensing Rh atoms with $^{16}O_2$ at 10–12 K, (A) Rh/$^{16}O_2 \simeq 1/10^3$ and (B) Rh/$^{16}O_2 \simeq 1/10^5$, showing the characteristic UV absorptions of $Rh(O_2)_2$ (M_2)[4] and $Rh_2(O_2)_4$ (D_4).

(on the 1076-cm^{-1} line of D_4) with D_3 is correct, then one can assign the overlapping isotopic structure of D_3 in the 1150–950-cm^{-1} region (Figure 5) in $^{16}O_2/^{18}O_2/Ar \simeq 1/1/100$ matrices as follows (cm^{-1}): (D_3) $Rh_2(^{16}O_2)_3$, 1080; $Rh_2(^{16}O_2)_2(^{18}O_2)$, 1048; $Rh_2(^{18}O_2)_3$, 1019; (M_2) $Rh(^{16}O_2)_2$, 1048; $Rh(^{16}O_2)(^{18}O_2)$, 1003; $Rh(^{18}O_2)_2$, 990. One concludes, therefore, that a coherent and logical set of assignments can be extracted from the $^{16}O_2$, $^{16}O_2/^{18}O_2$, $^{16}O_2$/Ar, and $^{16}O_2/^{18}O_2$/Ar experiments if one assumes the existence of four binuclear dioxygen complexes of the type $(O_2)_2Rh\text{-}Rh(O_2)_2$ (D_4), $(O_2)_2Rh\text{-}Rh(O_2)$ (D_3), $(O_2)Rh\text{-}Rh(O_2)$ (D_2), and $(O_2)Rh\text{-}Rh$ (D_1) (with the proposed absence of the geometrical isomer $Rh\text{-}Rh(O_2)_2$) coexisting with the known mononuclear complexes $Rh(O_2)_2$ (M_2) and $Rh(O_2)$ (M_1) with at least one "unique" (high-frequency) binuclear complex, $Rh_2(O_2)$ (D_1'), and at least one trinuclear complex, $Rh_3(O_2)_{2\text{ or }6}$ (T). Attempts to obtain further information about higher clusters in this system proved to be a fruitless task and so the remainder of the discussion in this paper will concentrate on the more reliable aspects of the eight complexes listed above.

UV-Visible Experiments. When Rh atoms are cocondensed with $^{16}O_2$ matrices under conditions which favor large amounts of $Rh_2(O_2)_4$ (Rh/$^{16}O_2 \simeq 1/10^3$), one observes a very intense UV transition centered around 250 nm with a noticeable low-energy shoulder at approximately 300 nm (Figure 6A). For the purpose of comparison we include the UV spectrum assigned to $Rh(O_2)_2$ (M_2, in part 1 of this study), obtained with Rh/$^{16}O_2 \simeq 1/10^5$ (Figure 6B). Evidence for weak absorptions in the range 400–900 nm could not be found for either compound. From a series of Rh/$^{16}O_2$ concentration experiments we conclude that band overlap occurs in the region of 250 nm for $Rh_2(O_2)_4$ (D_4) and $Rh(O_2)_2$ (M_2) and that two UV absorptions at 250 and 300 nm can be associated with the former compound. The origin of these electronic transitions is discussed later on.

Table III. Calculated and Observed Infrared-Active Isotopic Frequencies for $Rh_2(^{16}O_2)_n(^{18}O_2)_{4-n}$ (where n = 0-4)

Obsd ν, cm^{-1}	Calcd[a] ν, cm^{-1}	Assignment
1078	1078.7	$Rh_2(^{16}O_2)_4$
1051	1054.2	$Rh_2(^{16}O_2)(^{18}O_2)_3$[b]
1045	1039.0	$Rh_2(^{16}O_2)_2(^{18}O_2)_2$[b]
1024	1027.1	$Rh_2(^{16}O_2)_3(^{18}O_2)$[b]
1018	1017.0	$Rh_2(^{18}O_2)_4$

[a] Calculated frequencies are based on a pseudotetrahedral model and a frequency factored force field, where the best fit between observed and calculated ν(OO) modes occurs for k_{OO} = 5.79 and $k_{OO,OO}$ = 0.31 mdyn/Å. [b] In phase modes calculated at 1181.3, 1167.8, and 1150.9 cm^{-1}, respectively. Not observed because of expected low intensity (see ref 7).

Discussion

Rhodium–rhodium bonds in the chemistry of low oxidation state rhodium are quite common. In the context of the following discussion, we note particularly the diamagnetic rhodium–rhodium bonded carboxylates $Rh_2(OOCR)_4L_2$ which have the well-known tetrabridged structure[8] and the nonbridged rhodium–rhodium bonded complexes $Rh_2(DMGH)_4(PPh_3)_2$[9] and $Rh_2(en)_4(H_2O)_2$.[10] It is also pertinent to note that rhodium complexes containing symmetrical triangular Rh_3 cluster residues have figured prominently in recent discussions of carbonyl scrambling processes, as exemplified by the isomers of $(\eta^5\text{-}C_5H_5)_3Rh_3(CO)_3$.[11]

Tetradioxygendirhodium, $Rh_2(O_2)_4$. In pure O_2 and concentrated O_2/Ar matrices, species D_4 forms readily at high Rh/matrix ratios. The quantitative Rh/O_2 concentration experiments establish D_4 to be the highest stoichiometry binuclear rhodium dioxygen complex formed under these conditions. Moreover, its facile generation on warming matrices rich in $Rh(O_2)_2$ to 30–40 K would indicate that the formulation $Rh_2(O_2)_4$ is a plausible a priori stoichiometric assignment for D_4.

The simplicity of the infrared spectrum of $Rh_2(O_2)_4$ in the oxygen–oxygen stretching region, namely, a single, sometimes split, absorption (1083/1078 cm^{-1}) depending on the matrix deposition conditions, is suggestive of a highly symmetrical structural unit. On these grounds the existence of a bridging tetrasuperoxo structure in pure O_2 matrices seems unlikely,[12] while a metal–metal bonded entity $(O_2)_2Rh\text{-}Rh(O_2)_2$ (consistent with the idea of being the dimer of the parent $Rh(O_2)_2$) is an entirely reasonable structure.[9-11,18,21] Assuming that the dioxygen moieties bond in a side-on fashion to the rhodium atoms in $(O_2)_2RhRh(O_2)_2$, as would appear to be the case in $Rh(O_2)_2$, then structures differing in the relative orientation of the "$Rh(O_2)_2$ residues" with respect to each other are possible candidates for D_4. Obviously a number of different rotameric forms are possible, and three of these are shown below:

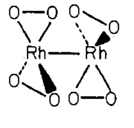
C_{2h}

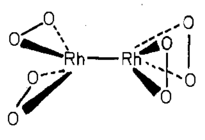
D_{2d}

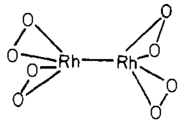
D_{2h}

For the cases shown, one expects two infrared-active ν(OO) stretching modes. In practice, however, a single (or slightly split) ν(OO) absorption is observed indicating symmetry close to spherical (pseudotetrahedral). The observation of a *quintet* $^{16}O_2/^{18}O_2$ isotope pattern for $(O_2)_2Rh\text{-}Rh(O_2)_2$ is certainly not inconsistent with this idea (Table III). The reasonably close agreement between the observed and calculated ν(OO) stretching frequencies, based on a point mass Rh_2 approximation and a frequency-factored force field (Table III), would tend to support the pseudotetrahedral $(O_2)_2Rh\text{–}Rh(O_2)_2$ model. We note also that the 40-cm^{-1} "blue shift" in the $\nu(OO)$ stretching mode on passing from $Rh(O_2)_2$ to $(O_2)_2Rh\text{–}Rh(O_2)_2$ is the trend expected on forming a Rh–Rh bonded dimer species, that is, Rh to O_2 charge transfer decreases in the dimer compared to the monomer because of the electron density requirements of the metal–metal bond.

Finally it is relevant to note that Dubicki and Martin[18] recently undertook an SCCC–MO calculation on $Rh_2(OAc)_4(H_2O)_2$ in an effort to understand the electronic structure, diamagnetism, and Rh–Rh bonding in the complex. Their interpretation was consistent with a closed shell configuration and a formulation of the metal–metal bonding as single (σ), arising from the configuration $[(\pi^4)(\sigma)^2(\delta)^2(\delta^*)^2(\pi^*)^4]$. A Rh–Rh bond order of unity is certainly consistent with the reported Rh–Rh distance of 2.39 Å[19] and is considerably longer than the Mo–Mo distance of 2.11 Å in $Mo_2(OAc)_4$[20] where a strong quadruple bond is believed to exist. On the basis of Dubiki and Martin's[18] molecular orbital calculations for $Rh_2(OAc)_4(H_2O)_2$ and the sensitivity of the UV–visible spectrum of the diaquo species to changes in the terminal ligands, they ascribed an intense UV absorption at roughly 250 nm to a $\sigma\text{–}\sigma^*$ type transition, between orbitals associated with the Rh–Rh bonding.[5] It should be noted that this absorption is roughly two orders of magnitude *more intense* than the visible transitions observed around 600 and 450 nm.[18,21] By experimenting in pure O_2 matrices, under Rh/O_2 conditions which favored the production of large quantities of $Rh_2(O_2)_4$ (described earlier), we observed an intense UV absorption centered at 250 nm, with a low-energy shoulder at roughly 300 nm. These spectral features dominated the spectra on deposition at 10–12 K and after warmup to 35 K. Weak absorptions in the visible region of the spectrum could not be detected even when the 250-nm line was arranged to be two linear absorbance units. Therefore, on concluding this discussion, we would like to propose that the similarity of the UV spectra of $Rh_2(O_2)_4$, $[Rh_2(H_2O)_{10}]^{4+}$, $[Rh_2(CO_3)_4]^{4-}$, and $Rh_2(OAc)_4(H_2O)_2$[18,21] provides evidence in favor of a metal–metal bonded $Rh_2(O_2)_4$ complex. Moreover, in view of our extended Hückel analysis of $Rh(O_2)_2$ and $Pd(O_2)_2$ described in part 1 of this study and a systematic study of the charge-transfer spectra of $M(O_2)_2$ species (where M = Ti, V, Cr, Mn, Fe, Co, Ni, Cu),[24] we would propose that the 250-nm band of $Rh_2(O_2)_4$ is best assigned to an $O_2 \rightarrow Rh$ charge-transfer transition with the 300-nm band associated with the expected $\sigma\text{–}\sigma^*$ type transition[18,21] between orbitals associated primarily with the Rh–Rh bond of $Rh_2(O_2)_4$.

Chemisorbed Oxygen on Rhodium Metal Surfaces: Localized Bonding Models. One of the most striking features of recent (LEED) structural determinations of oxygen chemisorbed on well-defined rhodium (100) and (110) metal surfaces is the relatively large number of observed O–O separations falling in the range 2.14–3.21 Å.[13] All O–O distances are considerably larger than those observed for O–O bonds (1.21–1.49 Å) but generally fall in the range expected for chemisorbed structures (2.14–3.21 Å), ionic crystals (2.29–3.25 Å), and covalent species (2.09–2.60 Å).[13] Generally speaking, these results are representative of most room temperature chemisorption studies of oxygen on rhodium surfaces and display all of the features expected for dissociatively chemisorbed dioxygen with phase oxide nucleation occurring under severe conditions such as anodization.[14]

The literature on this subject reveals a severe lack of spectroscopic data for the molecular form of chemisorbed dioxygen on rhodium (as well as iridium[15]) surfaces. However, it is probably not unfair to suppose that "small" amounts of associatively chemisorbed dioxygen, which could be the active component in certain heterogeneous oxidation catalysis processes, may be found in future low-temperature photoemission (LEED) and other surface spectroscopic studies.[23,25] It is therefore possible that our spectroscopic results for $Rh_x(O_2)_y$ complexes might have some bearing on rhodium-catalyzed oxidation processes induced by transient $Rh(O_{2chemi})$ molecular surface species. We note briefly that propylene oxidation by Ir/SiO_2-supported catalysts yields mainly acetaldehyde and has been interpreted[16] as involving a surface $Ir(O_{2chemi})$ species and a reactive intermediate in which the propylene adds across the coordinated dioxygen surface molecule as shown below:

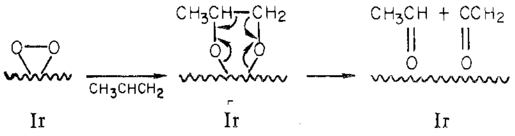

(In view of ref 25, this now seems to be a reasonable mechanism.) On the other hand, Rh/SiO_2-supported catalysts[17] convert propylene mainly to acrolein and water, through a proposed symmetric reaction intermediate $(\ddot{C}H_2\text{–}\ddot{C}H\text{–}\ddot{C}H_2)$. However, the surface oxygen species responsible for this process has not been ascertained.

In relating our data for $Rh_x(O_2)_y$ complexes to dioxygen chemisorbed on rhodium surfaces, we would like to propose the following. Let us assume that only one dioxygen ligand can bond in a terminal (side-on or end-on) fashion to a Rh surface site. Under these circumstances we would contend that complexes D_1 and D_2 may be useful "localized bonding" models for associatively chemisorbed dioxygen on rhodium surfaces at low dioxygen coverages.

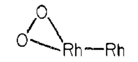

(D_1, 922 cm^{-1})

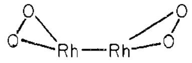

(D_2, 902 cm^{-1})

The small $\nu(OO)$ frequency shift on passing from D_1 to D_2 (20 cm^{-1}) and the close similarity of these $\nu(OO)$ frequencies to that observed for $Rh(O_2)$ imply minimal nearest-neighbor dioxygen coupling effects, minimal perturbation effects of adding a second Rh atom, and therefore an argument in favor of using these reactive intermediates as models for $Rh(O_{2chemi})$. Extending these ideas to the "high coverage" reactive intermediates D_3 and D_4 one can see that the $\nu(OO)$ stretching mode of the "$Rh(O_2)_2$" residues are again very similar and shifted only 38–41 cm^{-1} from $Rh(O_2)_2$ itself, thereby providing further support for the validity of a localized bonding approach to associative dioxygen chemisorption.

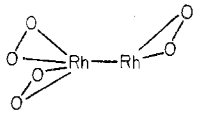

(D_3, 1081 cm^{-1})

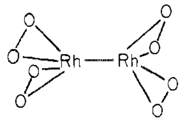

(D_4, 1076 cm^{-1})

The existence of the "unique" binuclear complex $Rh_2(O_2)$, D_1', and its remarkably high $\nu(OO)$ stretching mode at 1278–1266 cm^{-1} force one to invoke a different type of rhodium–dioxygen interaction from that proposed for $Rh_2(O_2)$, D_1. Clearly the degree of rhodium-to-dioxygen charge transfer in D_1' is considerably less than that in D_1, the latter being best described as $Rh_2^{\delta+}(O_2^{\delta-})$ where $1 < \delta < 2$. One may extrapolate this idea to D_1' and propose the description $Rh_2^{\delta+}(O_2^{\delta-})$ with $0 < \delta < 1$. D_1' may therefore be considered as a localized bonding model for "physisorbed" O_2 on rhodium surfaces, involving two rhodium atom sites as shown below:

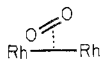

D_1, on the other hand, may be more akin to the strongly chemisorbed form of O_2 which, under the working conditions of a supported Rh catalyst, could be considered to be a "model precursor" for dioxygen dissociation and oxide formation.

By proposing a very weak rhodium dioxygen interaction in D_1', one must be alert to the idea that more than one dioxygen could in fact be associated with the Rh_2 moiety, because $^{16}O_2/^{18}O_2$ isotopic substitution would be expected to be relatively insensitive to dioxygen–dioxygen vibrational coupling effects.

Turning our attention finally to the interesting trinuclear species T we note particularly (i) the $\nu(OO)$ stretching frequency occurs in the range that we attribute to "$Rh(O_2)_2$" residues (see D_3, D_4, M_2), (ii) the trimer forms readily when O_2 matrices rich in $Rh(O_2)_2$ and $Rh_2(O_2)_4$ are warmed to 40 K, (iii) the $\nu(OO)$ frequency order follows the trend $T > D_4 > M_2$, and (iv) the $^{16}O_2/^{18}O_2$ isotopic data suggest a possible bis(dioxygen) formulation $Rh_3(O_2)_2$, although it would be difficult to distinguish $Rh_3(O_2)_2$ from a $Rh_3(O_2)_6$ complex (weak dioxygen–dioxygen coupling) with the available isotopic data. With the knowledge that trinuclear metal cluster compounds containing triangular metal cluster residues are quite common[11] and have often been proposed as useful chemisorption models for the triangular M_3 surface atom groupings in hcp and ccp metals,[1] we will assume that this structural arrangement is an appropriate description for our trinuclear rhodium cluster and that we are dealing in pure O_2 matrices with $Rh_3(O_2)_2$ or $Rh_3(O_2)_6$. Intuitively we favor the latter formulation on the grounds that the associated $\nu(OO)$ stretching mode appears in the range which we have ascribed to "$Rh(O_2)_2$" residues and moreover completes the expected $\nu(OO)$ trend $T > D_4 > M_2$. Further detailed studies will be required to establish whether a

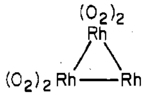

formulation is correct and representative (together with its reactive intermediates $Rh_3(O_2)_n$ where $n = 1–5$) of the chemisorbed state of O_2 on the threefold sites of rhodium-metal surfaces.

Acknowledgment. This work was completed while G. A. O. was a Sherman-Fairchild Distinguished Scholar (1977) at California Institute of Technology. The hospitality of the Chemistry Division of Caltech is greatly appreciated. We gratefully acknowledge the financial assistance of the National Research Council of Canada, the Atkinson Foundation, the Connaught Fund, Imperial Oil of Canada, the Lash Miller Chemistry Laboratory, and Erindale College. An NRCC scholarship awarded to A.J.L.H. is also appreciated.

Registry No. D_1, 63866-64-8; D_1', 63866-63-7; D_2, 63866-62-6; D_3, 63866-61-5; D_4, 63866-60-4; M_1, 63848-54-4; M_2, 63904-17-6; $Rh_2(^{16}O_2)(^{18}O_2)_3$, 63866-58-0; $Rh_2(^{16}O_2)_2(^{18}O_2)_2$, 63866-69-3; $Rh_2(^{16}O_2)_3(^{18}O_2)$, 63866-68-2; $Rh_2(^{18}O_2)_4$, 63866-67-1; $Rh_2(^{16}O_2)_2(^{18}O_2)$, 63866-66-0; $Rh_2(^{18}O_2)_3$, 63866-65-9; $Rh(^{16}O_2)(^{18}O_2)$, 63866-48-8; $Rh(^{18}O_2)_2$, 63866-47-7; $Rh_3(O_2)_2$, 63937-02-0; $Rh_3(O_2)_6$, 63866-59-1.

References and Notes

(1) (a) E. Drauglis and R. I. Jaffee, Ed., "The Physical Basis of Heterogeneous Catalysis", Plenum Press, London–New York, 1975; R. B. Anderson and P. T. Dawson, Ed., "Characterization of Surfaces and Adsorbed Species", Vol. 3, Academic Press, New York, N.Y., 1976; R. C. Baetzold, *Adv. Catal.*, **25** (1976); J. C. Bucholz and G. A. Somorjai, *Acc. Chem. Res.*, 9, 333 (1976), and references therein; (b) R. P. Messmer, S. K. Knudson, K. H. Johnson, J. B. Diamond, and C. Y. Yang, *Phys. Rev. B*, **13**, 1396 (1975); R. P. Messmer in "Physical Basis for Heterogeneous Catalysis", E. Drauglis and R. I. Jaffee, Ed., Plenum Press, New York, N.Y., 1975; K. H. Johnson and R. P. Messmer, *Int. J. Quant. Chem., Symp.*, **10**, 147 (1976); N. Rösch and K. H. Johnson, *Phys. Today*, 34 (1974); C. F. Melius, J. W. Moskowitz, A. P. Mortola, M. B. Baillie, and M. A. Ratner, *Surf. Sci.*, **59**, 279 (1976); N. Rösch and T. N. Rhodin, *Faraday Discuss. Chem. Soc.*, **58**, 28 (1974); I. P. Batra and O. Robaux, *J. Vac. Sci. Technol.*, **12**, 242 (1975); A. Anderson, *J. Am. Chem. Soc.*, **99**, 696 (1977); *J. Chem. Phys.*, **65**, 1729 (1976); **64**, 4046 (1976); *Chem. Phys. Lett.*, **35**, 498, 2975 (1976); G. Blyholder, *Surf. Sci.*, **42**, 249 (1974); A. Anderson and R. Hoffmann, *J. Chem. Phys.*, **61**, 4545 (1974); H. F. Schaefer III, *Acc. Chem. Res.*, **10**, 287 (1977); W. A. Goddard, G. A. Ozin, W. J. Power, and T. Upton, *J. Am. Chem. Soc.*, in press, and references therein; (c) R. Ugo, *Catal. Rev.*, **11**, 225 (1975); E. L. Muetterties, *Bull. Soc. Chem. Belg.*, **84**, 959 (1975); **85**, 7 (1976); G. A. Ozin, *Acc. Chem. Res.*, **10**, 21 (1977); T. E. Madey, J. T. Yates, Jr., D. R. Sandstron, and R. J. H. Voorhoevre in "Treatise on Solid State Chemistry", Vol. 6B, B. Hannay, Ed., Plenum Press, New York, N.Y., 1976, p 1; L. H. Little "Infrared Spectra of Adsorbed Species", Academic Press, London, 1966; M. L. Hair, "Infrared Spectroscopy in Surface Chemistry", Marcel Dekker, New York, N.Y., 1967; J. E. Demuth and D. E. Eastman, *Phys. Rev. Lett.*, **32**, 1123 (1974); J. E. Demuth, *Chem. Phys. Lett.*, **45**, 12 (1977); H. Conrad, G. Ertl, H. Knözinger, J. Küppers, and E. E. Latta, *Chem. Phys. Lett.*, **42**, 115 (1976); G. C. Bond, "Catalysis by Metals", Academic Press, London–New York, 1962, and references therein; (d) E. L. Muetterties, *Science*, **196**, 839 (1977), and references therein.

(2) See for example R. Busby, W. Klotzbücher, and G. A. Ozin, *J. Am. Chem. Soc.*, **98**, 4013 (1976); W. Klotzbücher and G. A. Ozin, *Inorg. Chem.*, **16**, 984 (1977); and references therein.

(3) G. A. Ozin, *Catal. Rev.*, in press; M. Moskovits and G. A. Ozin in "Cryochemistry", Wiley, New York, N.Y., 1976.

(4) A. J. L. Hanlan and G. A. Ozin, *Inorg. Chem.*, preceding paper in this issue.

(5) $X\alpha$-SW calculations on $Rh_2(O_2CH)_4(H_2O)_2$ confirm the Dubicki–Martin occupation scheme and proposal of a single Rh–Rh bond; they also agree with the assignment of the 250-nm band to a $\sigma \rightarrow \sigma^*$ transition (J. G. Norman, Jr., personal communication).

(6) E. P. Kündig, M. Moskovits, and G. A. Ozin, *Nature (London)*, **254**, 503 (1975); M. Moskovits and J. Hulse, *J. Chem. Soc., Faraday Trans. 2*, 471 (1977).

(7) H. Huber, W. Klotzbücher, G. A. Ozin, and A. Vander Voet, *Can. J. Chem.*, **51**, 2722 (1973); J. Darling, M. B. Garton-Sprenger, and J. S. Ogden, *Faraday Soc. Symp.*, **8**, 75 (1973).

(8) F. A. Cotton, *J. Am. Chem. Soc.*, **92**, 2926 (1970).

(9) K. G. Caulton and F. A. Cotton, *J. Am. Chem. Soc.*, **93**, 1914 (1971).

(10) R. D. Gillard, B. Heaton, and D. V. Vaughan, *J. Chem. Soc. A*, 734 (1971).

(11) R. J. Lawson and J. R. Shapley, *J. Am. Chem. Soc.*, **98**, 7434 (1976), and references therein.

(12) T. B. Freedman, C. M. Yoshida, and T. M. Loehr, *J. Chem. Soc., Chem. Commun*, 1016 (1974), and references therein.

(13) C. W. Tucker, Jr., *J. Appl. Phys.*, **37**, 4147 (1966), and references therein.

(14) D. A. J. Rand and R. Woods, *J. Electroanal. Chem.*, **31**, 29 (1971).

(15) G. Broden and T. N. Rhodin, *Faraday Discuss. Chem. Soc.*, **60**, 112 (1975), and references therein; J. Küppers and A. Plagge, *J. Vac. Sci. Technol.*, **13**, 259 (1976).

(16) N. W. Cant and W. K. Hall, *J. Catal.*, **27**, 70 (1972).

(17) N. W. Cant and W. K. Hall, *J. Catal.*, **22**, 287 (1971); *J. Phys. Chem.*, **75**, 2914 (1971).

(18) L. Dubicki and R. C. Martin, *Inorg. Chem.*, **9**, 673 (1970).

(19) F. A. Cotton, B. G. DeBore, and M. D. LaPrade, *Acta Crystallogr., Sect. B*, **27**, 1664 (1971).

(20) J. V. Bencic and F. A. Cotton, *Inorg. Chem.*, **8**, 7 (1969).

(21) C. R. Wilson and H. Taube, *Inorg. Chem.*, **14**, 405 (1975); F. Maspero and H. Taube, *J. Am. Chem. Soc.*, **90**, 7361 (1968).

(22) C. Leung and R. Gomer, *Surf. Sci.*, **59**, 638 (1976).

(23) In this context we note that dioxygen chemisorption on, for example, tungsten is generally considered to be dissociative. However, at $T < 40$ K it has recently been demonstrated that dioxygen adsorbs in a "molecular" form,[22] from which the more strongly bound, atomic chemisorption state seen at high temperature is derived. Similar effects have been observed for dihydrogen on tungsten (see Ehlich in ref 22) and it would appear that the phenomenon of molecular precursors to atomic adsorption is fairly widespread. These surface molecules may turn out to be closely related to the $Rh_x(O_2)_y$ localized bonding models of the present study.

(24) H. B. Gray, A. J. L. Hanlan, A. B. P. Lever, G. A. Ozin, and W. J. Power, in preparation.

(25) We note with great interest that low-temperature (–70 to –100 °C) thermal desorption studies of oxygen chemisorbed onto single-crystal (100) iridium surfaces show the presence of *both* molecular dioxygen and atomic oxygen species, the former apparently transforming to the latter on warming above –70 °C. The existence of an associatively chemisorbed, molecular dioxygen precursor on iridium was kindly brought to our attention by Professor H. Weinberg and Mr. J. Taylor of Caltech at the galley proof stage of this manuscript (personal communication).